

Atom Lithography using MRI-type feature placement

J. H. Thywissen* and M. Prentiss†

Department of Physics, Harvard University, Cambridge, Massachusetts 02138, USA

(Dated: November 4, 2018)

We demonstrate the use of frequency-encoded light masks in neutral atom lithography. We demonstrate that multiple features can be patterned across a monotonic potential gradient. Features as narrow as $0.9\mu\text{m}$ are fabricated on silicon substrates with a metastable argon beam. Internal state manipulation with such a mask enables continuously adjustable feature positions and feature densities not limited by the optical wavelength, unlike previous light masks.

Atom lithography has been used to make lines as small as 13nm [1, 2], to fabricate features with aspect ratios greater than 2:1 [3, 4], and to pattern areas as large as 38cm^2 [5]. Atoms patterned with light masks are uniquely well-suited for structured doping [6] and for fabrication demanding long-range coherence [7]. However, feature spacings in light masks have been limited by the length scale of the optical wavelength used [8, 9, 10, 11, 12, 13, 14, 15, 16, 17, 18]. In this Letter, we demonstrate a technique that extends light masks beyond the feature density of optical lithography and to more complex patterns than standing wave interferences.

Research in neutral atom lithography has been motivated by several considerations. Neutral atomic beams with thermal kinetic energies have short ($< .1\text{nm}$) de Broglie wavelengths, minimizing diffractive resolution limitations. Neutral atoms are insensitive to stray electric and magnetic fields, and long-range inter-particle interactions are weak. A wealth of atom optics (mirrors, guides, etc.) have been developed, including light masks, which, unlike physical masks, do not sag and cannot be clogged or damaged. Laser-accessible internal structure of atoms allows efficient cooling, the storage of internal energy, and complex manipulations. State-sensitive atom lithography with metastable atoms has been demonstrated with both positive- and negative-tone resists capable of sub-10-nm resolution [5, 19, 20].

In this work we encode the desired position distribution using the *frequency*, instead of the intensity, of the light. In the presence of an appropriate potential gradient, the optical resonant frequency of the atom will be position-dependent. Thus each spectral component of a laser beam interacts with the atoms at a specific but separate location. The frequency encoding of spatial information is commonly known from magnetic resonance imaging (MRI), where protons (instead of atoms) are imaged (instead of patterned) in a potential gradient by radio- (instead of optical-) frequency radiation. We will refer to atom lithography with frequency-encoded light masks as Atomic Resonance Lithography (ARL). Thomas and coworkers have developed neutral atom measurement techniques based on a more direct analogue to MRI [21, 22].

Frequency encoding has several promising features.

Just as sub- $100\text{-}\mu\text{m}$ features can be resolved with 100-meter wavelength radio waves in MRI, far sub-optical (ie, sub-micron) features and spacings can be created with optical resonances in atoms [21, 22, 23]. As shown in Ref. [23], arbitrary patterns can be frequency-encoded and generated. Furthermore, ARL can create two-dimensional patterns, just as MRI can image two- [24] or three-dimensional distributions. Finally, frequency-encoded masks do not demand high transverse coherence of the incident atoms. By contrast, although intricate holographic patterns [25, 26, 27] have been detected, the required coherent sources lack the flux to pattern a surface: experiments have used integrated surface densities on the order of 10^9 below a typical lithographic dose.

Figure 1 describes a realization of ARL based on quenching directly within the potential gradient. First, metastable argon atoms are optically pumped to the

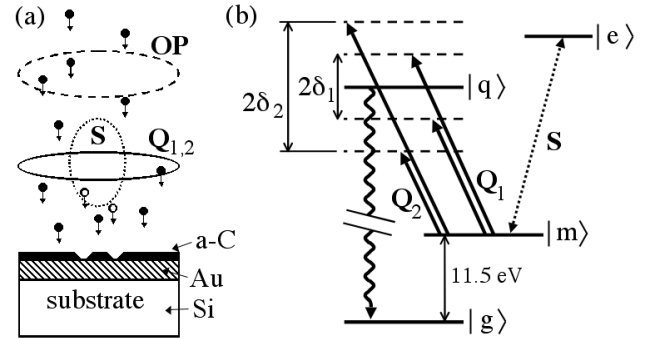


FIG. 1: The first of two light masks used for atomic resonance lithography. (a) Argon atoms strike a gold surface after passing through a sequence of laser beams (not to scale) propagation parallel to the surface: optical pump **OP**, shift **S**, and quench **Q**. The light mask selectively quenches some atoms to their ground state $|g\rangle$ (open circles), in which state atoms are unable to activate the formation of resist on the surface. At all other locations, metastable atoms $|m\rangle$ (filled circles) activate the growth of carbonaceous resist (a-C) on the substrate. (b) Level diagram relevant to **S** and **Q**. An on-resonant light shift beam (**S**) is applied on a cycling transition between the metastable state $|m\rangle$ and excited state $|e\rangle$. Two pairs of detunings (Q_1 and Q_2 , detuned $\pm\delta_1$ and $\pm\delta_2$, respectively) excite atoms to $|q\rangle$, from which atoms decay, in a radiative cascade, to the inert ground state $|g\rangle$.

$|J = 2, m_J = 2\rangle$ sublevel of the $4s[3/2]_2^o$ or $1s_5$ state. Not shown is earlier optical quenching of the atoms in the $4s'[1/2]_0^o$ or $1s_3$ state. If unquenched, these “J=0” atoms would contribute a background rate of resist formation. Next, the atoms pass through a zone of two overlapping beams. A resonant σ^+ “shift” beam (S) on the 812 nm $|J = 2, m_J = 2\rangle \rightarrow |J' = 3, m_{J'} = 3\rangle$ cycling transition overlaps with a σ^- “quench” beam (Q) containing four frequency components, $\pm\delta_1$ and $\pm\delta_2$. As shown in Fig. 2a, these frequencies are resonant at two stark shifts (i.e., four positions) in the resonant shift beam. At these four positions, atoms are optically pumped by Q to the true atomic ground state $|g\rangle$. Note that two frequencies (e.g., $\pm\delta_1$) were required for complete optical pumping at each resonant position because atomic population existed at both the strong- and weak-field-seeking dressed states. This internal state manipulation creates a pattern on a surface by exploiting the internal energy difference between the the ground state and the $4s[3/2]_2^o$ metastable state of argon: atoms in $|m\rangle$ release 11.5 eV of internal energy to activate the formation of a resist on the surface (as described below), while atoms in $|g\rangle$ do not affect the surface. Thus, the detunings δ_1 and δ_2 control where features – here, stripes of unprotected surface – will appear.

Metastable argon (Ar*) atoms exposed the substrate through the light mask with a flux density of $3 \times 10^{12} \text{ cm}^{-2} \text{ s}^{-1}$. Because the system is evacuated with diffusion pumps, surfaces within the system are covered with several monolayers of siloxane hydrocarbons. When the metastable atoms hit the surface, they transfer their internal energy to the physisorbed hydrocarbons and induce a chemical change that results in the formation of a durable material. The resist material remains on the surface even after exposure to air and/or solution, and can thus be used as a mask for etching. The beam apparatus and lithographic process used in this work have been described in more detail elsewhere [5].

A gold substrate was exposed for five hours through the optical mask of Fig. 1. The light mask parameters were as follows. The S beam had 5.9 mW cylindrically focused to a profile of $46 \mu\text{m}$ by $925 \mu\text{m}$, creating a maximum stark shift that was spectroscopically measured to be 150 MHz. Cylindrically symmetric 110- μm -wide quench beams Q₁ and Q₂ each had 70 μW of power, split between the pair of detunings, $\pm\delta_1 = \pm 2\pi \times 40 \text{ MHz}$ and $\pm\delta_2 = \pm 2\pi \times 110 \text{ MHz}$. After exposure, the substrate was removed from the vacuum system and etched for 7 minutes in a ferricyanide solution.

Figure 2b shows an optical micrograph of the etched substrate. At positions where either Q₁ or Q₂ was resonant, metastable atoms were quenched, leaving the underlying substrate unprotected against the subsequent gold etch. At all other positions, a resist material was formed as described above, and gold remained on the silicon substrate after etching. A pattern was formed across 2 cm of the substrate. Figure 2b was taken in the cen-

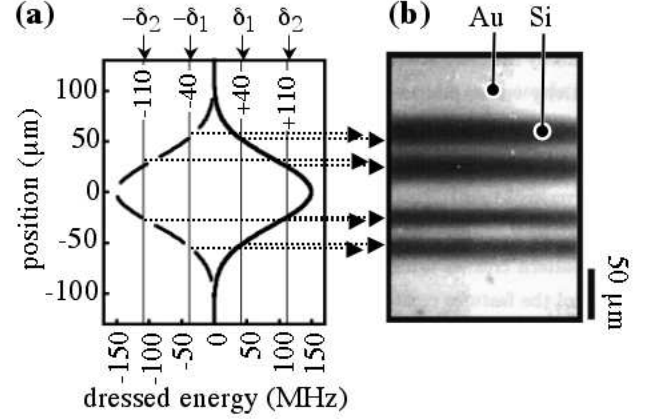


FIG. 2: (a) Energy times $1/h$ versus position of the weak-field-seeking (solid line) and strong-field-seeking (dashed line) dressed states of an atom in the S beam. Thin solid lines show the quench detunings $\pm\delta_1$ and $\pm\delta_2$ (b) Optical micrograph of a gold-on-silicon substrate after exposure and etch. The dark lines are exposed silicon, and correspond to locations where atoms were quenched, thus preventing the formation of a resist and allowing gold to be etched. These features are formed at resonant quench locations, as indicated by dotted arrows between (a) and (b).

ter of that pattern, where atoms entered perpendicular to the light mask. The comparison (indicated by dotted arrows) to Fig. 2a shows that, as desired, there are four features: two on each side of the Gaussian intensity profile of the S beam. We fit the sum of four Lorentzians to the integrated reflectivity profile of the substrate to determine more precise feature locations and positions. The lower (upper) two lines have a half-width of $10 \pm 1 \mu\text{m}$ ($14 \pm 1 \mu\text{m}$) and a center-to-center separation of $26 \pm 2 \mu\text{m}$ ($34 \pm 2 \mu\text{m}$). The asymmetry between the upper and lower set of lines was not expected, but could be explained by aberrations in the cylindrical optics that formed the shift beam. The lower set of lines are within experimental error of the expected linewidth of atomic density, $9 \mu\text{m}$ (as discussed below), and the expected feature separation, $27 \mu\text{m}$. Note that the transfer function from atomic flux density to reflectivity of the surface after etching is nonlinear, such that purely atomic calculations may vary systematically from the observed features.

The significance of the result shown in Fig. 2 is that two lithographic features were created across each monotonic part of the potential. Unlike previous atom lithographic results with light masks, *the wavelength of light does not determine the minimum feature separation*. The ultimate resolution of ARL can be limited by a variety of effects, discussed Refs. [21, 23] and summarized in the following paragraphs.

The most fundamental limitation is the spectroscopic precision with which each resonant transfer position is defined, $\delta x_{\text{sp}} = \hbar\Gamma'/F$, where Γ' is the spectroscopic width of the transition, and F is the potential gradient. In these

experiments we used laser light to create the potential gradient, but gradients could also be created with magnetic [22] or electric fields. For the realization of ARL discussed above, Γ' is the power-broadened and time-broadened quenching transition, with a natural linewidth $\Gamma = 2\pi \times 5$ MHz. Experimentally, $\Gamma' = 2\pi \times 20$ MHz. For the gradient $F/\hbar = 2\pi \times 2.3$ MHz/ μm at the feature locations in Fig. 2, we find $\delta x_{\text{sp}} = 9 \mu\text{m}$. Note that for a Raman transition, as will be considered below, $\Gamma' = v_L/w_0 = 1/\tau$, where $v_L = 850$ m/s is the longitudinal velocity of the Ar^* atoms, w_0 is the $1/e^2$ intensity waist of the Raman beams, and τ is the atom-light interaction time.

Atomic motion during the transfer can also limit the resolution. While transferring an atom of mass M to a state with a gradient F , acceleration and diffraction limit the resolution to the order of $F\tau^2/2M$, where τ is again the transfer time [21]. However, the numerical factors depend on which states are in a gradient and for how long. In the case where Γ' is determined by the interaction time of a Raman transfer, and the pattern is formed by the atoms transferred to the gradient, one can choose an optimal τ to give a resolution of $\delta x_\ell = 2(\hbar^2/2MF)^{1/3}$. For ^{40}Ar and $F/\hbar = 2\pi \times 1$ MHz/ μm , the optimal size is $\delta x_\ell = 100$ nm. This limit is not, however, fundamental: Olshanii *et al.* show that an appropriate choice of probe frequency variation during atomic transfer (a “magic phase”) can correct for later evolution, such that the spectroscopic resolution δx_{sp} is recovered [23].

Free flight between the pattern formation and the substrate will allow the atoms to diffract further. Given a free-flight time T_{FF} , the diffraction limit is $\delta x_{\text{dif}} = \sqrt{\hbar T_{FF}/2M}$. For instance, for $T_{FF} = 30\Gamma^{-1}$, this limit is $\delta x_{\text{dif}} = 27$ nm, smaller than the other limits given here. Note that this is a quantitative restatement of one of the desirable qualities of atoms as a patterning constituent: their short de Broglie wavelength λ_{dB} minimizes the diffraction, $\sim \sqrt{\lambda_{dB}D}$, where D is the mask-substrate separation.

The collimation of the atomic beam can limit the resolution of the pattern. Given an rms velocity spread v_{rms} , $\delta x_v \approx v_{\text{rms}}(\tau + T_{FF})$. For $\tau + T_{FF} = 30\Gamma^{-1}$ and $v_{\text{rms}} = 0.5$ m/s, $\delta x_v = 0.4 \mu\text{m}$. Thus with a small (20 nm) transverse coherence length, sub-micron lithography can be performed.

In order to improve our resolution, we performed a second experiment with several experimental modifications. First, we improved the quality of the optics forming the **S** beam to reduce the waist by a factor of 3. Next, as shown in Fig. 3, we used a coherent transfer scheme by detuning the **S** beam by 2 GHz and introducing Raman beams. At resonant positions in the light mask, the Raman beams transfer atoms from $|m1\rangle$ to $|m2\rangle$. In the third interaction zone, only the atoms transferred to $|m2\rangle$ are quenched [28]. With such a scheme, we realized a

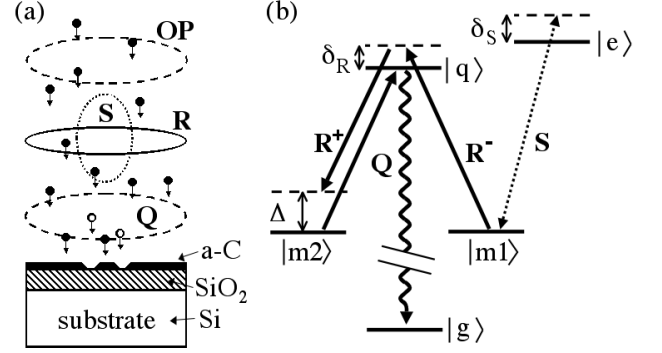


FIG. 3: ARL light mask using two-photon transfer and dark states. (a) The geometrical arrangement of the light mask. The substrate consists of a 15 nm silicon-dioxide layer over a bulk silicon layer. (b) Atoms are prepared in the state $|m1\rangle$ (optical pump transition not shown). At locations where the Stark shift of the **S** beam matches the differential detuning Δ of the Raman beams (**R**⁺ and **R**[−]), atoms are transferred to $|m2\rangle$. In the subsequent quenching zone, atoms in $|m2\rangle$ are optically pumped to $|g\rangle$ by **Q**.

factor of 10 improvement in resolution, as described below. Furthermore, such a coherent ARL scheme avoids momentum diffusion by spontaneous emission, and can implement further resolution improvements such as the coherent manipulations described in Ref. [23].

A silicon $\langle 100 \rangle$ substrate with a 15 nm oxide layer was exposed for six hours through the ARL mask depicted in Fig. 3. The **R** beam of $25 \mu\text{m}$ by $103 \mu\text{m}$ had σ^- and σ^+ components with powers of $65 \mu\text{W}$ and $60 \mu\text{W}$ and detunings of $+61.1$ MHz and $+104.2$ MHz, respectively. A 1.3 G quantization field reduced the differential detuning by 5.4 MHz, such that the net Raman detuning was $\Delta/2\pi = -37.7$ MHz. The shift beam **S** was detuned by $\delta_S/2\pi = 2.00$ GHz above resonance, had 6.9 ± 0.3 mW of power, and a profile of $15 \pm 1 \mu\text{m}$ by $250 \mu\text{m}$. The σ^+ polarized **S** beam interacted with both $|m1\rangle$ and $|m2\rangle$, but gave a differential gradient $F/\hbar = 2\pi \times 6.4$ MHz/ μm due to the difference in Clebsch-Gordan coefficients: 1 and $\sqrt{2/5}$, respectively (note that Fig. 3 shows only the transition $|m1\rangle - |e\rangle$, for simplicity). The third interaction zone had a $350 \mu\text{W}$ quench beam (**Q**) with a waist of $210 \mu\text{m}$, such that about 12 photons are scattered from atoms in $|m2\rangle$. Because $|m1\rangle$ was in the $|2, +2\rangle$, it was dark with respect to the σ^+ polarized quench. Untransferred atoms arrived at the substrate in the metastable state $|m1\rangle$, and could therefore activate resist formation on the substrate.

After exposure, the pattern was transferred to the substrate using both dry and wet etches. First, the sample was etched for 35 s in a CHF_3 reactive ion etch with parameters 42 mTorr chamber pressure, 100 W forward power, 10 W reflected power, -842 V self-bias, and 25.0 sccm flow rate. Second, the sample was etched for

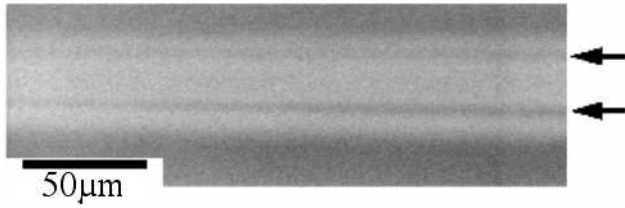


FIG. 4: SEM image of a Si (100) substrate patterned by the light mask shown in Fig. 3. The darker lines (indicated by arrows) are places at which metastable atoms were quenched, thus preventing the formation of a resist material and allowing the silicon to be etched.

50 s in 2% HF to prepare an unoxidized silicon face. Finally, the sample was etched for 14 min in 20% KOH at 22 C [4].

Figure 4 shows a scanning electron micrograph of the etched sample. The features created by ARL are indicated by arrows. Two features are created with a single Raman detuning because the Stark shift is equal to Δ at a location to either side of its maximum. The dark lines against a bright background indicate places at which silicon was preferentially etched. The sample was patterned across several millimeters of length. At center, for the run parameters above (gradient $F/\hbar = 2\pi \times 6.4 \pm 0.5 \text{ MHz}/\mu\text{m}$ and $\tau = 29 \pm 2 \text{ ns}$), the expected feature separation is $19.0 \pm 1.5 \mu\text{m}$, and the spectroscopic limit is $\delta x_{\text{sp}} = 0.86 \pm 0.07 \mu\text{m}$. This agrees well with our measurements: a minimum spacing of $(20.0 \pm 0.4) \mu\text{m}$ and a rms width of $(0.9 \pm 0.1) \mu\text{m}$.

These fabricated features are thirty times smaller than those that have been detected in holographic masking experiments [26], but still two orders of magnitude larger than the smallest features fabricated with atom lithography [1, 2, 3, 4]. Were the light gradient to be increased, feature sizes in the second ARL scheme demonstrated would be limited by the velocity spread of the atomic beam, at $\delta x_v = 0.4 \mu\text{m}$. Therefore, the spectroscopically limited feature size observed in Fig. 4 is a factor of two above the minimum observable linewidth for the collimation of our atomic beam. By comparison, the resolution limit of an optimized light mask with a gradient of $F/\hbar = 2\pi \times 6.4 \text{ MHz}/\mu\text{m}$ is $\delta x_\ell = 54 \text{ nm}$ for Ar*.

In conclusion, we have demonstrated the use of frequency encoding in optical masks for atom lithography. Using a two-photon internal state transfer, we create features in silicon with an rms width of $0.9 \pm 0.1 \mu\text{m}$. With a mask based on optical pumping, we show that feature position can be chosen continuously throughout monotonic potential gradients. Such a method could be used to form intricate, sub-micron, two-dimensional patterns with currently available sources. Lithography using internal ma-

nipulation schemes could also be extended to alkali atoms by state-selective ionization and deflection. Unionized alkali atoms, like unquenched metastable atoms, would be left to pattern an atom resist (e.g., [29]).

The authors thank N. Dekker and K. S. Johnson for contributions to the early stages of this project. We also thank F. Altarelli, G. Zabow, and S. Coutreau for assistance. This work was supported in part by the NSF Grant No. PHY-9876929, MRSEC Grant No. DMR-9809363, and the Hertz Foundation.

* email: joseph.thywissen@post.harvard.edu

† email: prentiss@fas.harvard.edu

- [1] R. E. Behringer *et al.*, J. Vac. Sci. Technol. B **14**, 4072 (1996).
- [2] W. R. Anderson *et al.*, Phys. Rev. A **59**, 2476 (1999).
- [3] S. J. Rehse *et al.*, Appl. Phys. Lett. **71**, 1427 (1997).
- [4] J. H. Thywissen *et al.*, J. Vac. Sci. Technol. B **16**, 1155 (1998).
- [5] K. S. Johnson *et al.*, Appl. Phys. Lett. **69**, 2773 (1996).
- [6] T. Schulze *et al.*, App. Phys. Lett. **78**, 1781 (2001).
- [7] J. H. Thywissen *et al.*, J. Vac. Sci. Tech. B **16**, 3841 (1998).
- [8] G. Timp *et al.*, Phys. Rev. Lett. **69**, 1636 (1992).
- [9] J. J. McClelland *et al.*, Science **262**, 877 (1993).
- [10] R. W. McGowan, D. M. Giltner, S. A. Lee, Opt. Lett. **20**, 2535 (1995).
- [11] R. Gupta *et al.*, Appl. Phys. Lett. **67**, 1378 (1995); U. Drodofsky *et al.*, Appl. Phys. B **65** 755 (1997).
- [12] Features spaced by $\lambda/8$ were created in R. Gupta *et al.*, Phys. Rev. Lett. **76**, 4689 (1996).
- [13] U. Drodofsky *et al.*, Microelectron. Eng. **35**, 285 (1997).
- [14] F. Lison *et al.*, App. Phys. B **65** 419 (1997).
- [15] K. S. Johnson *et al.*, Science **280**, 1583 (1998).
- [16] P. Engels *et al.*, App. Phys. B **69**, 407 (1999).
- [17] B. Brezger *et al.*, Europhys. Lett. **46**, 148 (1999).
- [18] M. Mützel *et al.*, Phys. Rev. Lett. **88**, 083601 (2002).
- [19] K. K. Berggren *et al.*, Science **269**, 1255 (1995).
- [20] S. B. Hill *et al.*, App. Phys. Lett. **74**, 2239 (1999).
- [21] J. E. Thomas, Opt. Lett. **14**, 1186 (1989); J. E. Thomas, Phys. Rev. A **42**, 5652 (1990); J. E. Thomas, L. J. Wang, Physics Reports **262**, 311 (1995).
- [22] K. D. Stokes *et al.*, Phys. Rev. Lett. **67**, 1997 (1991); J. R. Gardner *et al.*, Phys. Rev. Lett. **70**, 3404 (1993).
- [23] M. Olshanii *et al.*, Phys. Rev. A **62**, 033612 (2000).
- [24] P. C. Lauterbur, Nature **242**, 190 (1973).
- [25] J. Fujita *et al.*, Nature **380**, 691 (1996).
- [26] M. Morinaga *et al.*, Phys. Rev. Lett. **77**, 802 (1996).
- [27] F. Shimizu, Adv. Atom. Mol. Opt. Phys. **42**, 73 (2000).
- [28] Whether to quench $|m1\rangle$ or $|m2\rangle$ depends on the tone of the resist and type of pattern desired.
- [29] K. K. Berggren *et al.*, Adv. Mater. **9**, 52 (1997); M. Kreis *et al.*, Appl. Phys. B **63**, 649 (1996).